Machine Learning and RBF Interpolation on Nanofluid Flow in a Rounded Corner Cavity

Merve Gurbuz-Caldag[1] and Bengisen Pekmen[2]

Abstract— In this study, three machine learning techniques and RBF interpolation are compared on a heat transfer and fluid flow problem in a cavity having rounded corner through the left bottom corner. The two dimensional, time dependent dimensionless governing equations of the problem are numerically solved by the radial basis function (RBF) method for space derivatives and by the backward Euler method for time derivatives. The differentially heated cavity has straight hot left wall and cold right wall, the top wall is the adiabatic wall and the bottom wall involving the rounded corner is the insulated wall. The numerical results show that the presence of the rounded corner causes convective heat transfer to increase. A dataset involving inputs as Rayleigh number and the radius of the circular corner and output as the average Nusselt number along the hot left wall is collected from the numerical results. The machine learning techniques, neural networks, gaussian process regression and ensemble learning as well as RBF interpolation are deployed for modeling. Each modeling results in small mean squared error metric results, but the best modeling is found by RBF interpolation.

I. INTRODUCTION

A rounded corner cavity (rcc) provides smoother flow patterns, prevents stationary zones and diminishes flow separation unlike sharp corner cavities. This phenomena is used in the design of the cooling of circuit boards, solar air heaters and heat exchanger with grooves having rounded corners [1]. Ray and Misra [2] analyzed the friction factor and the heat transfer of a laminar flow in square cavity with rounded corners. It is reported that both the friction factor and the Nusselt number (Nu) increase at lower values of radius of the rounded corner. They also obtained the correlations of these parameters and compared with the numerical data. Entropy generation of natural convection flow in a rcc is investigated for different values of irreversibility and aspect ratios, Rayleigh number (Ra), and the radius of the corner by Salari et al. [3]. Entropy generation is a decreasing function of radius of corner but increasing function of the other physical parameters. Gurturk et al. [4] examined the impact of arc-shaped partitions on the natural convection flow. Two types of partitions are used as aluminum and wood. Both partitions eliminates the death zone obtained in the sharp corner. Inclined magnetic field effect is added to the mixed convection flow in a lid-driven rcc by Colak et al. [5]. Numerical computations are carried out for Richardson (Ri) and Hartmann (Ha) numbers, inclination angle (γ) and the radius of the corner. They showed that there is no significant effect of the radius of the corner on flow field except for $\gamma = \pi/4$. In [6], finite element method is implemented to magnetohydrodynamic (MHD) natural convection flow in a rcc with circular obstacle. The Nusselt number on the hot corner augments with an increasing size of the obstacle.

The influence of round corner on the convection flow including nanaoparticles is also investigated. Selimefendigil and Inada [7] considered the natural convection flow of SiO2-water nanofluid in square cavity with a conductivity partition located in the left upper corner. It is found that the rise in the size of the partition improves the heat transfer. They also obtained that the rate of the heat transfer of cylindrical shape of nanaoparticle is greater than spherical one. In [8], the heat transfer of Ag/MgO-water hybrid nanaofluid is studied in a cavity with a round corner including porous medium subjected to the magnetic field. Nu increases as the thickness of the porous medium but it decreases with the augmentation of Ha. Korei et al. [1] used OpenFOAM to MHD mixed convection flow in a rcc filled by Al2O3/Cu-water. They depicted that the heat transfer rate diminishes as the radius of the corner increases.

In recent years, machine learning approach has been implemented the heat transfer problems since this approach provides the predictive model with high accuracy and low computational cost. Vaferi et al. [9] compared the capability of artificial neural network (ANN) approaches to estimate convective heat transfer of nanofluids through a circular tube. Multi-layer perceptron neural network gives the best performance compared to the others. Hemmat Esfe and Afrand [10] demonstrated that ANN is an effective method for the prediction of thermal conductivity and thermal viscosity of the nanofluid. Kumar and Kavitha [11] implemented Gaussian process (GP) regression to estimate viscosity of Al_2O_3-water nanofluid. In [12], Bayesian Regularization technique of ANN is used to model the Nusselt number of Ag-MgO-water nanofluid in an amorphous cavity in the presence of magnetic field. Datasets are generated from the numerical results obtained by finite element method based on conrtol volume. Deymi et al. [13] applied ensemble model (EM) to predict the specific heat capacity of the

*This work was not supported by any organization

[1]Merve Gurbuz-Caldag is with the Department of Mathematics, TED University, Ankara, 06420, Turkey merve.gurbuz@tedu.edu.tr

[2]Bengisen Pekmen is with the Department of Mathematics, TED University, Ankara, 06420 , Turkey bengisen.pekmen@tedu.edu.tr

nanofluid. Pekmen Geridonmez and Oztop [14] model the global and local entropy generations of Cu-water nanofluid in a square cavity under the effect of oriented magnetic field by using NN. They found that the metric results of local entropy indicators are worse than global ones. In [15], the prediction of thermal and energy transport of hybrid nanofluids is investigated using GP. Li et al. [16] compared five ML models including EM to forecast condensation heat transfer coefficient. Pekmen Geridonmez [17] used the RBF interpolation and ANN to model heat transfer rate of natural convection flow with or without magnetic field.

Literature survey reveals that there is no reported work about the estimation of the average Nusselt number of Cu-water nanofluid in a square cavity with rounded corner by using different machine learning and interpolation techniques. Data are collected from the numerical results for input features in the range of Rayleigh number and the radius of the corner with the target, average Nusselt number. The novelty lies in the comparative evaluation of multiple modeling methods (NN, GP, EM, RBF) applied to a new physical scenario which is Cu-water nanofluid convection in a rounded corner cavity. In the following parts, the problem definition, a brief description of computational approaches, and modeling results are presented, respectively.

Nomenclature

Latin Symbols

r_c	radii of rounded corner
L	Characteristic length
p	Pressure
u	x-component of the velocity of the fluid
v	y-component of the velocity of the fluid
Ra	Rayleigh number
ρ	Fluid density
T	Temperature
T_c	Temperature of cold wall
T_h	Temperature of hot wall
$\bar{Nu}$	Average Nusselt number
ψ	Stream function
ω	Vorticity
g	Gravitational acceleration
ΔT	Temperature difference

Greek Letters

α	Thermal diffusivity
β	Thermal expansion coefficient
ϕ	Solid volume fraction
ν	Kinematic viscosity
μ	Dynamic viscosity

Subscripts

f	Fluid
nf	Nanofluid
s	Solid

II. DEFINITION OF THE PROBLEM

The two-dimensional, time dependent natural convection flow of Cu-water nanofluid flow in a unit square cavity having rounded corner with radius r_c is investigated. The demonstration of the problem is presented in Fig. 1. The vertical straight walls from left to right are hot (T_h) and cold (T_c) walls, respectively, while the other walls are adiabatic.

The effect of buoyancy force is treated by Boussinesq approximation because of the temperature difference resulting with density difference. The viscous dissipation and the radiation effect are neglected.

The single phase model for nanofluid is picked, and therefore the physical properties are stated by [18]

$$\rho_{nf} = (1-\phi)\rho_f + \phi\rho_s, \tag{1}$$

$$(\rho c_p)_{nf} = (1-\phi)(\rho c_p)_f + \phi(\rho c_p)_s, \tag{2}$$

$$(\rho\beta)_{nf} = (1-\phi)(\rho\beta)_f + \phi(\rho\beta)_s, \tag{3}$$

$$\alpha_{nf} = \frac{k_{nf}}{(\rho c_p)_{nf}}, \tag{4}$$

where subindices nf, f, s are the nanofluid, fluid and solid, respectively, ρ is the density, β is the thermal expansion coefficient, c_p is the specific heat, α is the thermal diffusivity and ϕ is the solid volume fraction. The thermal (k_{nf}) conductivity of the nanofluid are settled as [19]

$$\frac{k_{nf}}{k_f} = \frac{k_s + 2k_f - 2\phi(k_f - k_s)}{k_s + 2k_f + \phi(k_f - k_s)}, \tag{5}$$

and the dynamic viscosity of nanofluid μ_{nf} is opted as [20]

$$\mu_{nf} = \mu_f(1-\phi)^{-2.5}. \tag{6}$$

Thermophysical properties of water and copper (Cu) are tabulated as in Table I.

TABLE I

Thermophysical properties of water and Cu.

Property	Water	Cu
ρ (kg/m^3)	997.1	8933
c_p $[J/(kgK)]$	4179	385
k $[W/(mK)]$	0.613	401
$\beta \times 10^{-5}$ $(1/K)$	21	1.67

The physical equations [21] as a combination of continuity, momentum and energy may be written as

$$\nabla \cdot \mathbf{u} = 0, \tag{7a}$$

$$\nu_{nf}\nabla^2\mathbf{u} = \frac{\partial \mathbf{u}}{\partial t} + (\mathbf{u}\cdot\nabla)\mathbf{u} + \frac{1}{\rho_{nf}}\nabla P + \frac{(\rho\beta)_{nf}}{\rho_{nf}}(T - T_c)\mathbf{g}, \tag{7b}$$

$$\alpha_{nf}\nabla^2 T = \frac{\partial T}{\partial t} + u\frac{\partial T}{\partial x} + v\frac{\partial T}{\partial y}, \tag{7c}$$

where $\mathbf{u} = \langle u, v\rangle$ is the velocity vector and $\mathbf{g}$ is the gravitational acceleration vector, T is the temperature, p is the pressure, $\nu = \mu/\rho$ is the kinematic viscosity.

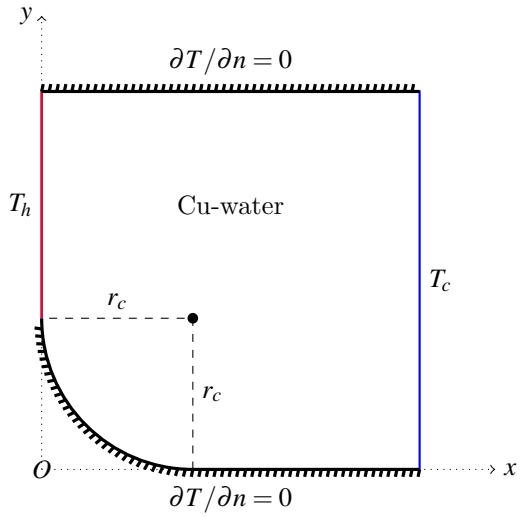

Fig. 1. The geometrical layout of the problem.

With the help of the stream function definition of velocity components $((u,v)=(\psi_y,-\psi_x))$, continuity equation is satisfied, and the definition of vorticity $(\omega = v_x - u_u)$ allows us to eliminate the pressure terms from the momentum equations. Thus, the stream function-vorticity form of equations are deduced as

$$\nabla^2\psi = -\omega \tag{8a}$$

$$\frac{\alpha_{nf}}{\alpha_f}\nabla^2 T = \frac{\partial T}{\partial t} + \left(u\frac{\partial T}{\partial x} + v\frac{\partial T}{\partial y}\right) \tag{8b}$$

$$\frac{\mu_{nf}}{\mu_f}Pr\nabla^2\omega = \frac{\rho_{nf}}{\rho_f}\left(\frac{\partial \omega}{\partial t} + u\frac{\partial \omega}{\partial x} + v\frac{\partial \omega}{\partial y}\right) - \frac{(\rho\beta)_{nf}}{\rho_f\beta_f}RaPr\frac{\partial T}{\partial x} \tag{8c}$$

where the nondimensional parameters are Prandtl number $(Pr = \nu_f/\alpha_f)$ and Rayleigh number $(Ra = \rho\beta_f\Delta T L^3/(\nu_f\alpha_f))$.

III. COMPUTATIONAL APPROACHES

A. RBF Method

The numerical part of the study is carried out by applying the global radial basis function (RBF) method to space derivatives and the backward Euler to time derivatives.

RBFs are functions depending on the radial (Euclidean) distance $r = \sqrt{(x-x_j)^2+(y-y_j)^2}$ between the collocation (x_j,y_j) and the field (x,y) points. The novel and concise books [22], [23] involve many theoretical and practical implementation examples on RBFs.

Any unknown φ may be written as a product of a coordinate matrix F constructed by an RBF and an unknown vector of coefficients. The partial derivatives of unknown is also easily derived by this product and by the straightforward derivative calculations of RBFs. The differentiation matrices for x-, y- derivatives and Laplacian are found as

$$D_x = \frac{\partial F}{\partial x}F^{-1}, D_y = \frac{\partial F}{\partial y}F^{-1}, D_2 = \left(\frac{\partial^2 F}{\partial x^2} + \frac{\partial^2 F}{\partial y^2}\right)F^{-1}, \tag{9}$$

Iterations are terminated if the sum of the relative residuals in infinity norm is less than a tolerance 10^{-5}. A relaxation parameter $\tau\,(0<\tau<1)$ is utilized once ω equation is solved.

Average Nusselt number along the heated straight left wall are computed from

$$\overline{Nu} = \frac{1}{1-r_c}\frac{k_{nf}}{k_f}\int_{r_c}^{1} -\frac{\partial T}{\partial x}dy, \tag{10}$$

using composite Simpson's rule on nonuniform grids [24].

B. Machine Learning and NN Approaches

1) Neural Network Regression: NN process works as feedforward NN [25] In this case, the information flows from the left to the right. The first layer is the input layer. The hidden layers follow the first layer, and the last layer is the output layer. A simple generalized mathematical expression may be written as

$$\hat{\mathbf{y}} = f(W\mathbf{x}+b), \tag{11}$$

where W is the weight matrix, b is the bias vector, $\mathbf{x}$ is the input features, $\hat{\mathbf{y}}$ is the predicted output, and f is the activation function.

In Matlab, 'fitrnet' is used for NN modeling.

2) Gaussian Process (GP) Regression: In this process kernel (covariance) functions play the significant role. The GP function $f(x)$ is expressed as [26], [27]

$$f(x) \approx GP(m(x),k(x,x')), \tag{12}$$

where $m(x) = E[f(x)]$ is the mean function, $k(x,x') = E[(f(x)-m(x))(f(x')-m(x'))]$ is the covariance function. In this study, ARD squared exponential kernel is taken as

$$k(x,x') = \sigma^2 \exp\left[-\frac{1}{2}\sum_{m=1}^{d}\frac{(x_m-x'_m)^2}{\sigma_l^2}\right], \tag{13}$$

where σ is the standard deviation, σ_l is the characteristic length scale, x,x' are input vectors of size $d\times 1$.

In Matlab, 'fitrgp' is used for GP modeling.

3) Ensemble Learning (Boosting): In this modeling, multiple weak learners, which are usually small decision trees, are combined to get a stronger model. In case of boosting, the process works sequentially correcting the errors from the previous learners, and the last model is a weighted sum of weak learners.

In mathematical terms, the general ensemble model (EM) is as follows [28]

$$\hat{y} = \sum_{m=1}^{M} w_m f_m(x), \tag{14}$$

where w_m is the weight, f_m is the m^{th} weak learner and M is the total number of weak learners.

4) RBF Interpolation: RBFs may also be used for interpolation, and in turn prediction by using interpolation. If the train data φ_{tr} is written as $\varphi_{tr} = F_{tr}\tilde{\alpha}$ with F_{tr} of size N_{tr}^2 and $\tilde{\alpha}$ is of size N_{tr}, where N_{tr} is the size of the train data, then the test data is predicted by

$$\varphi_t = F_t \tilde{\alpha}, \tag{15}$$

where F_t is the matrix of size $N_t \times N_{tr}$ and is constructed by the RBF function considering the radial distances between the test data points and the train data points.

RBF interpolation is utilized by $f = r^3$ in an in-house implementation in Matlab.

IV. MODELING RESULTS

The data are collected from the numerical results solving the problem in 109 different values of $Ra \in [1000, 10^5]$, and 20 distinct values of $r_c \in [0, 0.5]$. The target value is considered as average Nusselt number along the heated wall. That is, the first two columns of the data are input features Ra, r_c and the last column is the response value $\overline{Nu}$. The stored data as a matrix is of size 2180×3. The data is divided into 80% train and 20% test parts. In NN and GP modeling, the data is standardized. In the RBF interpolation, normalization in the first input column (in Ra values) is done. The EM modeling has no any data scaling. These data scalings are determined as the best fit cases. All variables required for NN, GP, EM, and RBF are given in Table II.

TABLE II
Configuration Parameters for NN, GP, EM, and RBF Models

Model	Implementation	Key Parameters
NN	fitrnet	• Architecture: 1 hidden layer • Neurons per layer: 50 • Activation function: ReLU
GP	fitrgp	• Kernel: ARD squared exponential
EM	fitrensemble	• Learner type: Decision Trees • Learning Cycles: 200 • Learning Rate: 0.1 • Boosting method: LSBoost
RBF	In-house	• Cubic PHS RBF (r^3) • Interpolation

Figure 2 depicts the modeling results of the estimation $\overline{Nu}$ using NN, GP, EM and RBF interpolation. The subfigures in the first column indicate a good fit for each model since the predicted values are close to the numerical data. In the second column, all models provide good predictions with low residuals. Moreover, the highest accuracy is obtained by RBF interpolation. The mean squared error (MSE) metric results can be ordered as $RBF < GP < EM < NN$ so that RBF interpolation shows the best performance.

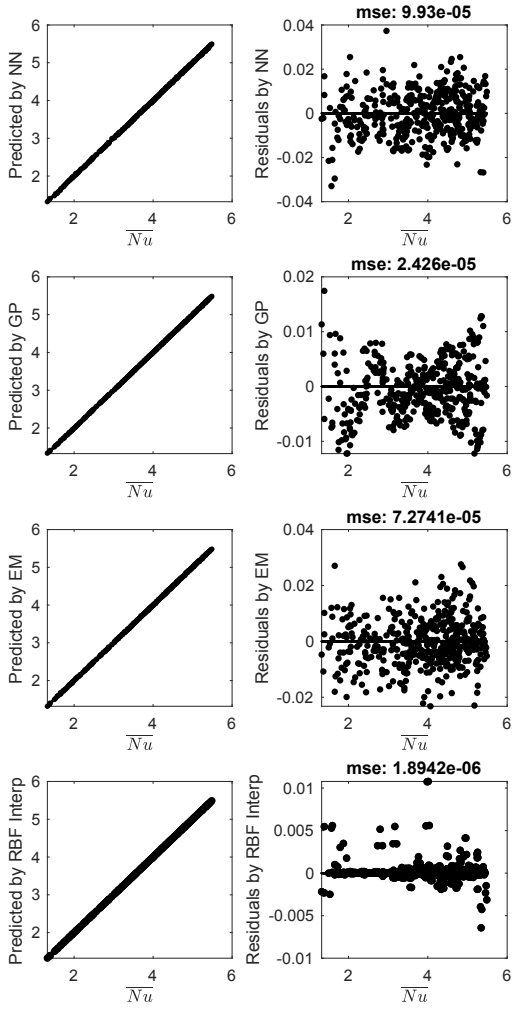

Fig. 2. Modeling results.

A. Physical Sense

Figures 3 and 4, show a systematic increase in $\overline{Nu}$ with both Ra and r_c. The mathematical structure of RBF interpolation aligns well with this physical behavior, as it naturally captures smooth, continuous relationships through distance-based interpolation. The data also reveals that $\overline{Nu}$ is highly sensitive to Ra but moderately sensitive to r_c. RBF interpolation can effectively handle inputs with different sensitivity scales without requiring extensive tuning, unlike NNs which might require careful architecture design.

The Ra values $(1000 - 100000)$ span two orders of magnitude while r_c values $(0 - 0.5)$ are much smaller. This scale difference also points why normalization suit well

for RBF interpolation, which relies on distance calculations.

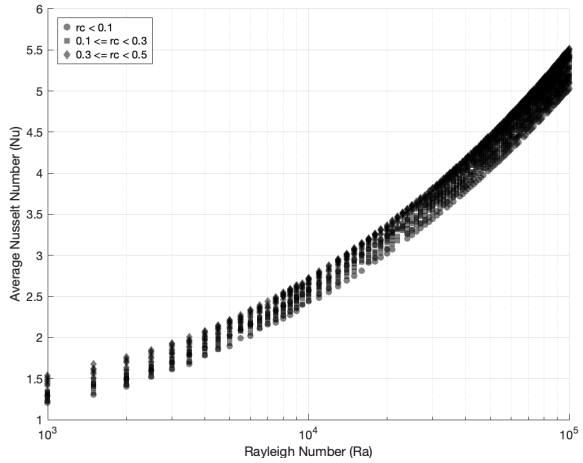

Fig. 3. Effect of Ra and r_c on average Nusselt number.

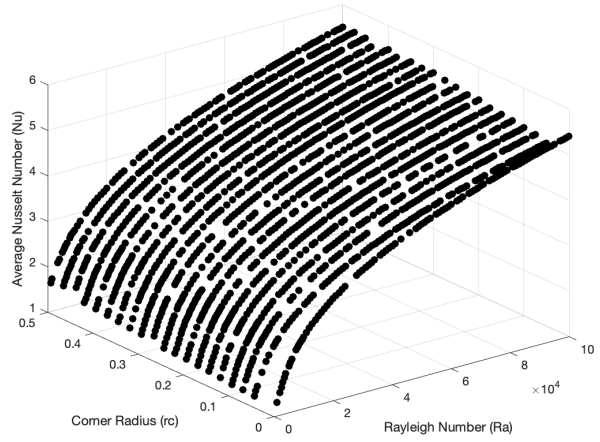

Fig. 4. 3D visualization of effect of Ra and r_c on average Nusselt number.

V. CONCLUSIONS

In this study, machine learning and RBF interpolation are investigated in a natural convection nanofluid flow problem inside a rounded corner cavity. The problem is numerically solved by RBF method in space derivatives and backward Euler in time derivatives. In different parameter variations of Rayleigh number and radius of the rounded corner, a data set is created involving these variations and the corresponding average Nusselt number values from the numerical calculations. Once the data is separated into train and test data, four models which are neural network, gaussian process regression, ensemble modeling and RBF interpolation are trained on train data, and then tested on test data. The mean squared error metric results demonstrates the good fit in each modeling. Nevertheless,RBF interpolation delivered the best results, achieving the lowest prediction error for the average Nusselt number. Compared to studies, this study combines numerical simulation with multiple data-driven modeling techniques to assess their performance in a domain with geometric complexity. The integration of physical simulation and learning-based approaches contributes to the development of accurate and computationally efficient approximate models for convection problems. However, this study has certain limitations. The nanofluid type (Cu-water) and cavity configuration are fixed, and the analysis is limited to two-dimensional laminar natural convection. In the future, we are planning to extend this work in several directions: applying the models to three-dimensional cavities, incorporating hybrid nanofluids, testing under different boundary conditions, and possibly integrating real-time control features. We also aim to explore other advanced modeling techniques, such as physics-informed neural networks, to further enhance accuracy and interpretability.

Appendix

Loaded Data in NN, GP, Emsemble

```
trainn = load('data_train.csv');
testt = load('data_test.csv');
```

NN, GP, Ensemble

```
models = fitrnet(trainn(:,1:2), trainn(:,colout),
'LayerSizes', Lsz,...
'Activations', 'relu', 'Lambda', 0, ...
'IterationLimit', 1000, 'Standardize', true);
```

```
models = fitrgp(trainn(:,1:2),trainn(:,colout), '
    Standardize', true, 'BasisFunction', '
    pureQuadratic','KernelFunction', '
    ardsquaredexponential');
```

```
models = fitrensemble(trainn(:,1:2),trainn(:,
    colout), 'Method', 'LSBoost','
    NumLearningCycles', 200 ,'LearnRate', 0.1,'
    Resample', 'on');
```

```
testpred = predict(models,testt(:,1:2)); % For
    Testing
```

RBF Interpolation

```
traindata = load('data_train.csv');
testdata = load('data_test.csv');

% some data savings
Xdata = traindata(:,1); % Ra column
Ydata = traindata(:,2); % rc column
Zdata = traindata(:,3);  % target

Xdatatest = testdata(:,1);
Ydatatest = testdata(:,2);
Zdatatest = testdata(:,3);
% normalization to [0,1] in Xtrain and Xtest data
Xdatasc = (Xdata - min(Xdata))/(max(Xdata)-min(
    Xdata));
Xdatat = (Xdatatest - min(Xdata))/(max(Xdata)-min(
    Xdata));
%%% scaled Xdata & YData in original data
```

```
data = [Xdatasc Ydata];
datainterp = [Xdatat Ydatatest];
%%% interpolation by cubic PHS RBF
Ztestfit = globalRbf2D(data,datainterp,Zdata,3);
```


Acknowledgment

This study was supported by 2224-A - Grant Program for Participation in Scientific Meetings Abroad of The Scientific and Technological Research Council of Turkey (TÜBİTAK).

References

[1] Z. Korei, S. Benissaad, F. Berrahil, and A. Filali, MHD mixed convection and irreversibility analysis of hybrid nanofluids in a partially heated lid-driven cavity chamfered from the bottom side, International Communications in Heat and Mass Transfer, vol. 132, p. 105895, 2022.

[2] S. Ray, and D. Misra, Laminar fully developed flow through square and equilateral triangular ducts with rounded corners subjected to H1 and H2 boundary conditions. International Journal of Thermal Sciences, vol. 49, pp.1763-1775, 2010.

[3] M. Salari, A. Rezvani, A. Mohammadtabar, and M. Mohammadtabar, Numerical study of entropy generation for natural convection in rectangular cavity with circular corners. Heat Transfer Engineering, vol. 36, pp.186-199, 2015.

[4] M. Gurturk, H. F. Oztop, F. Selimefendigil, and K. Al-Salem, Effects of Arc-Shaped Partitions in Corners of a Shallow Cavity on Natural Convection. Hittite Journal of Science and Engineering, vol. 6, pp. 17-23, 2019.

[5] E. Colak, H. F. Oztop, and O. Ekici, MHD mixed convection in a chamfered lid-driven cavity with partial heating. International Journal of Heat and Mass Transfer, vol. 156, p. 119901, 2020.

[6] M. Hamid, M. Usman, W. A. Khan, R. U. Haq, and Z. Tian, Characterizing natural convection and thermal behavior in a square cavity with curvilinear corners and central circular obstacles. Applied Thermal Engineering, vol. 248, p.123133, 2024.

[7] F. Selimefendigil, and A. A. Inada, Nanoparticle Shape Effect on Natural Convection in a Corner Partitioned Square Cavity, vol. 31, pp. 143-151, 2016.

[8] B. M. Amine, F. Redouane, L. Mourad, W. Jamshed, M. R. Eid, and W. Al-Kouz, Magnetohydrodynamics natural convection of a triangular cavity involving Ag-MgO/water hybrid nanofluid and provided with rotating circular barrier and a quarter circular porous medium at its right-angled corner. Arabian Journal for Science and Engineering, vol. 46, pp. 12573-12597, 2021.

[9] B. Vaferi, F. Samimi, E. Pakgohar, and D. Mowla, Artificial neural network approach for prediction of thermal behavior of nanofluids flowing through circular tubes. Powder technology, vol. 267, pp. 1-10, 2014.

[10] M. Hemmat Esfe, M. and Afrand, M. Predicting thermophysical properties and flow characteristics of nanofluids using intelligent methods: focusing on ANN methods. Journal of Thermal Analysis and Calorimetry, vol. 140, pp. 501-525, 2020.

[11] P. C. Mukesh Kumar, and R. Kavitha, Prediction of nanofluid viscosity using multilayer perceptron and Gaussian process regression. Journal of Thermal Analysis and Calorimetry, vol. 144, pp. 1151-1160, 2021.

[12] S. Nasir, A. S. Berrouk, T. Gul, and A. Ali, Develop the artificial neural network approach to predict thermal transport analysis of nanofluid inside a porous enclosure. Scientific Reports, vol. 13(1), p. 21039, 2023.

[13] O. Deymi, F. Hadavimoghaddam, S. Atashrouz, A. Abedi, A. Hemmati-Sarapardeh, and A. Mohaddespour, Employing ensemble learning techniques for modeling nanofluids' specific heat capacity. International Communications in Heat and Mass Transfer, vol. 143, p. 106684, 2023.

[14] B. Pekmen Geridonmez, H. F. and Oztop, A machine learning approach for entropy due to natural convection flow of a nanofluid under the uniform inclined magnetic field. Numerical Heat Transfer, Part B: Fundamentals, pp. 1-16, 2024.

[15] S. G. Krishna, M. Shanmugapriya, B. R. Kumar, and N. A. Shah, Thermal and Energy Transport Prediction in Non-Newtonian Biomagnetic Hybrid Nanofluids using Gaussian Process Regression. Arabian Journal for Science and Engineering, vol. 49(8), pp. 11737-11761, 2024.

[16] W. Li, G. Zhang, and D. Yang, Comparative study for flow condensation heat transfer in horizontal enhanced tubes based on machine learning. International Journal of Heat and Mass Transfer, vol. 224, p. 125330, 2024.

[17] B. Pekmen Geridonmez, Modeling of average Nusselt number by machine learning and interpolation techniques. ASME Journal of Heat and Mass Transfer, 146, 2024.

[18] K. Khanafer, K. Vafai, and M. Lightstone, Buoyancy-driven heat transfer enhancement in a two-dimensional enclosure utilizing nanofluids, International Journal of Heat and Mass Transfer, vol. 46, pp. 3639-3653, 2003.

[19] J. M. Garnett, Xii. Colours in metal glasses and in metallic films, Philosophical Transactions of the Royal Society of London. Series A, Containing Papers of a Mathematical or Physical Character, vol. 203, pp. 385–420, 1904.

[20] H. C. Brinkman, The viscosity of concentrated suspensions and solutions, The Journal of Chemical Physics, vol. 20, pp. 571–571, 1952.

[21] S. M. Aminossadati, and B. Ghasemi, Natural convection cooling of a localised heat source at the bottom of a nanofluid-filled enclosure, European Journal of Mechanics-B/Fluids, vol. 28, pp. 630-640, 2009.

[22] G. E. Fasshauer, Meshfree Approximation Methods with Matlab, World Scientific Publications, Singapore, 2007.

[23] G. E. Fasshauer and M. McCourt, , Kernel-based Approximation Methods using MATLAB, World Scientific Publications, Singapore, 2015.

[24] R. Khan, M. R. Hossain and S. Parvin, Numerical integration schemes for unequal data spacing, American Journal of Applied Mathematics, vol. 5, pp. 48–56, 2017.

[25] T. W.S. Chow, and S.-Y. Cho, Neural Networks and Computing, Imperial College Press, 2007.

[26] H. Li, Gaussian Process Regression, MSc Thesis, Imperial College London, London, 2018.

[27] Matlab, Kernel (Covariance) Function Options, Mathworks, 2024. https://www.mathworks.com/help/stats/kernel-covariance-function-options.html

[28] T. Hastie, R. Tibshirani and J. Friedman, The Elements of Statistical Learning, Springer, 2009.